

Exchange bias in Co-Cr₂O₃ nanocomposites: A possible candidate for overcoming superparamagnetism

P Anil Kumar* and K Mandal[#]

Magnetism Laboratory, S N Bose National Centre for Basic Sciences,
Block JD, Sector III, Salt Lake, Kolkata-700 098

*anil@bose.res.in

[#] kalyan@bose.res.in

Abstract

The possibility of using exchange bias in ferromagnetic-antiferromagnetic system to overcome the effect of superparamagnetism in small cobalt nanoparticles is explored. We have prepared Co-Cr₂O₃ nanocomposite powders using a chemical method. It is shown that this system is a possible combination for overcoming the effect of superparamagnetism in cobalt nanoparticles. The superparamagnetic blocking temperature of 3 nm particles has been increased above 350K. The choice of Cr₂O₃ is vital as its T_N is higher compared to other antiferromagnetic materials used for this purpose such as CoO. The field cooled and zero field cooled hysteresis measurements of the samples confirm the existence of exchange bias interaction in this system.

1. Introduction:

The possibility of achieving ultra high-density data storage system using magnetic particles as memory elements and their uses in medicine has recently enhanced the research activities in the area of magnetic nanomaterials [1-3]. These applications need the smallest possible magnetic particles for effective usage. But as the size of the magnetic grain is reduced below a critical size, the domain wall formation is not supported energetically and hence the single domain particles are developed. These single domain particles are of great physical interest as they show strikingly new phenomenon [4-6]. On further reduction of grain size, the anisotropy energy holding the particle magnetization in a particular direction becomes comparable to that of thermal energy. This makes the particle magnetization to flip in all possible directions. As a result of it; the individual particles loose its ferromagnetic behavior. This phenomenon, called superparamagnetism [7,8] limits the use of ultra fine particles for various applications. The superparamagnetic phenomenon presents quite an interesting physics to be studied. These include the study on relaxation of magnetization in superparamagnetic samples with the application of high frequency oscillating magnetic fields. To increase the blocking temperature, above which superparamagnetism starts, by using ferromagnetic-antiferromagnetic exchange bias [9-11] system is also an important topic of research in magnetism. Assuming the existence of an exchange interaction between the spins of FM and AFM material at the interface can qualitatively explain the existence of extra anisotropy energy in this system. This extra anisotropy energy turns out to be unidirectional favouring the alignment of FM magnetization in a single direction. When a field is applied in the temperature range $T_N < T < T_C$, the FM spins line up with the field, while the AFM spins remain random. When the sample is cooled to $T < T_N$ in the presence of the magnetic field, the AFM spins next to the FM align ferromagnetically to those of the FM (assuming ferromagnetic interaction). When the field is reversed, the FM spins start to rotate. However, for sufficiently large AFM anisotropy, the AFM spins remain unchanged. Therefore, the interfacial interaction between the FM/AFM spins at the interface, tries to align ferromagnetically the FM spins with the AFM spins at the interface. In other words, the AFM spins at the interface exert a microscopic torque on the FM spins, to keep them in their original position (ferromagnetically aligned at the interface). Therefore, the FM spins have one single stable configuration, i.e. the anisotropy is *unidirectional*. Thus, the field needed to reverse

completely an FM layer will be larger if it is in contact with an AFM, because an extra field is needed to overcome the microscopic torque. However, once the field is rotated back to its original direction, the FM spins will start to rotate at a smaller field, due to the interaction with the AFM spins (which now exert a torque in the same direction as the field). The material behaves as if there was an extra (internal) biasing field; therefore, the FM hysteresis loop is shifted in the field axis, i.e. *exchange bias*. Since this exchange bias phenomenon is unidirectional it can be used to successfully lock the magnetization of superparamagnetic particles in a single direction against to the thermal flipping. Hence this leads to the overcoming of superparamagnetic limit.

Though most studied are multi-layer systems; the polycrystalline powder systems do show considerable exchange bias effect [12]. Skumryev et al [9] have used the exchange bias effect to beat the superparamagnetic limit in Co-CoO multilayers. They have enhanced the blocking temperature of 4nm Co nanoparticles from 10K to around 290K. In the present work we have studied the effect of exchange bias on the superparamagnetism of cobalt nanoparticles embedded in Cr₂O₃ matrix. The choice of Cr₂O₃ facilitates the use of the exchange bias system above 300K. This leads to the non-zero hysteresis of fine cobalt particles at room temperature.

2.Experimental:

The Co-Cr₂O₃ nanocomposite powders were prepared by thermal decomposition of their combined salt solution. The calculated amounts of Co(NO₃)₂ · 6H₂O and Cr(NO₃)₃ · 9H₂O are taken so as to have the desired weight percentage of Co and Cr₂O₃ in the final product. The nitrate salts are then dissolved in ethylene glycol by stirring for 45 min separately. Both the solutions are then mixed and stirred while heating till it forms a gel like substance consisting of sols of Co and Cr₂O₃. The so formed gel is then reduced in hydrogen gas in an electric furnace at various temperatures for different durations. The change in the heat treatment affects the size of the nanocomposites obtained. The samples presented in this paper are divided into 2 series. The samples with Co to Cr₂O₃ weight ratio of 30:70 are termed as Series I, while that with Co to Cr₂O₃ weight ratio of 40:60 are in Series II. Samples A, B and C forms series I and Sample D alone forms series II. The description of heat treatments for all the samples is given in Table.I along with the particles sizes calculated from XRD. X-ray diffractometer (PANalytical Xpert Pro) with Cu anode

has been used to study the phase and crystallite size of the samples. The HRTEM images have been recorded using JEOL 2100 model Electron Microscope at an electron accelerating voltage of 200kV. The selected area electron diffraction (SAED) has also been used to determine the crystal structure.

The magnetization measurements were carried out using SQUID magnetometer (Quantum Design, MPMS). The field cooled (FC) hysteresis loops were measured after cooling the sample in the presence of an external magnetic field of 30 kOe. Before applying the cooling field, the sample was heated to 350K. The zero field cooled (ZFC) hysteresis loops were measured after cooling the sample from 350K to the measuring temperature (50K and 300K) in absence of any external field. In both FC and ZFC cases the magnetic hysteresis loop was measured up to a maximum field of 20 kOe. For FC and ZFC magnetization versus temperature measurements, the cooling of the samples (in case of FC) and magnetic measurements were performed in presence of 100 Oe magnetic field.

3. Results and Discussions:

The XRD patterns obtained for different samples are shown in Figure.1. The patterns show the formation of cubic Co and rhombohedral Cr₂O₃ phases separately. The crystallite size increases with the increase in temperature and/or duration of heat treatment during reduction processes as observed in Fig.1. The crystallite size was calculated from Scherrer's formula [13] for Co and Cr₂O₃. The values are presented in Table.1 for all the samples.

The HRTEM images of A and C, shown in Figure.2, confirm the formation of nearly spherical nanoparticles. However, it is not clear from the images, if Co-Cr₂O₃ is forming a core-shell system. Hence we assume that there are two possibilities, core-shell structure and Co nanoparticles in a uniform Cr₂O₃ matrix. As both are equally probable, the sample can be a mixture of these two possibilities. The estimated size of different samples from HRTEM images matches with that obtained from XRD using Scherrer's formula.

The FC and ZFC hysteresis loops of samples A, B, C and D are shown in Figures 3(a), 3(b), 3(c) and 3(d) respectively at temperatures 50K and 300K. For clarity, magnified plots of hysteresis loops at lower fields are shown in the figures while their insets show the full hysteresis loops from -2T to 2T. All the samples show non-zero hysteresis loss at both

temperatures. The existence of exchange bias in the samples and if it is effective in overcoming the superparamagnetic limit of fine Co nanoparticles (particularly in case of Samples B and D) is to be verified from these measurements.

The existence of exchange bias between ferromagnetic Co and antiferromagnetic Cr_2O_3 systems can be verified by the shift of hysteresis loop along field axis in FC configuration. The origin of this loop shift has already been explained qualitatively in the introduction part. In all the four cases this kind of loop shift is observed at 50K in FC configuration (Figure.3). The amount of shift in hysteresis loop termed as exchange bias field (H_{EB}) is determined and presented in Table.1 along with the coercivity field H_{C} . Maximum H_{EB} of 427 Oe is observed in case of sample C. However, the value of H_{EB} in the present case is less compared with the corresponding values usually observed in multi-layer systems. At 50K, the enhancement of H_{C} value is observed in FC case (except in case of Sample B) compared to that for ZFC samples. Both the shifting of loop and enhancement of H_{C} indicate the presence of exchange bias between the Co and Cr_2O_3 interfaces. Samples B and D are of special interest as these samples consist of Co particles whose T_{B} is well below room temperature [14]. But our measurements show that these samples are not superparamagnetic even at 300K. So the superparamagnetic effect in fine Co particles is overcome using exchange bias effect. The observation is similar to that reported by Skumryev et al [9] as mentioned before. We have made use of the fact that Neel temperature T_{N} of Cr_2O_3 is higher ($\sim 310\text{K}$ for bulk Cr_2O_3) than of CoO ($\sim 290\text{K}$).

From the FC and ZFC M Vs T curves shown in Figure.4 it is clear that the blocking temperature is around or above 350K. In exchange biased systems the blocking temperature of ferromagnetic phase is influenced by the Neel temperature of antiferromagnetic phase. Enhancement of Neel temperature of Cr_2O_3 with decrease in particle size has been reported earlier [15]. Hence the observed higher T_{B} of the samples is in accordance with the T_{N} value for Cr_2O_3 .

Though various efforts were made earlier to enhance the blocking temperature using exchange bias [16, 17], the present work deals with the lower particle sizes of a few nm and yet provides a mechanism for obtaining a T_{B} above room temperature. In addition, the method used for sample preparation is very simple and cost effective. Hence the present system can be a competent possibility for the application in magnetic data storage systems.

However, the system has to be synthesized in layered form and the possibility of increasing cobalt percentage is to be checked in order to attain higher data storage densities.

4. Conclusions:

We have demonstrated the exchange bias effect in Co-Cr₂O₃ nanocomposite powders, prepared by a simple chemical method. The system seems to be an ideal choice for applications in magnetic data storage, due to high thermal stability of fine particle magnetization. Moderate coercivity values facilitate the easy writing of the data on the bits. However, the thin film form of the composite has to be prepared and tested for its feasibility.

Acknowledgements:

This work was supported by BRNS, Govt. of India under the project grant 2003/37/13/BRNS. One of the author (PAK) thanks CSIR, Govt. of India for the research fellowship.

References:

- [1] Martín, J.I.; Nogués, J.; Kai Liu; Vicent, J.L.; Ivan K. Schuller. 2003, *J. Magn. Magn. Mater.*, **256**, 449.
- [2] Shouheng Sun, Murray, C.B., Dieter Weller, Liesl Folks, Andreas Moser, 2000 *Science*, **287**, 1989.
- [3] Häfeli, U.; Schütt, W.; Teller, J.; Zborowski, M. (eds) *Scientific and Clinical Applications of Magnetic Materials*; Plenum, New York, 1997.
- [4] Chakraverty S., Mitra S., Mandal K., Nambissan P.M.G. and Chattopadhyay S., 2005, *Phys. Rev.B*, **71**, 024115.
- [5] Mandal K.; Mitra S.; Anil Kumar P., 2006 *Europhys. Lett.*, **75**, 618.
- [6] Ngo A. N., Bonville P. and Pileni M. P., 2001 *J. Appl. Phys.*, **89**, 3370.
- [7] Muroi M., Street R., McCormick P.G. and Amighian J., 2001, *Phys. Rev. B*. **63**, 184414.
- [8] Chakraverty S., Mandal K., Mitra S., Chattopadhyay S. and Kumar S., 2004, *Jpn. J. Appl. Phys.*, **43**, 7782.
- [9] Skumryev, V. Stoyan Stoyanov, Yong Zhang, George Hadjipanayis, Dominique Givord and Josep Nogués. 2003, *Nature*, **423**, 850.
- [10] Meiklejohn, W.H.; Bean, C.P., 1956, *Phys. Rev.*, **102**, 1413.
- [11] Nogués, J. & Schuller, I.K., 1999, *J. Magn. Magn. Mater.*, **192**, 203.
- [12] Meiklejohn, W.H. & Bean, C.P., 1957, *Phys. Rev.*, **105**, 904.
- [13] Mandal K., Chakraverty S., Pan-Mandal S., Agudo P., Pal M., and Chakravorty D., 2002, *J. Appl. Phys.* **92**, 501.
- [14] Jung Yup Yang, Kap Soo Yoon, Young Ho Do, Ju Hyung Kim, Jong Hyun Lee, Chae Ok Kim, Jin Pyo Hong and Eun Kyu Kim., 2005, *IEEE Trans. Magn*, **41**, 3313-3315.
- [15] Hou, B., Ji. X., Xie, Y., Li, J., Shen, B. and Qian, Y., 1995, *Nanostruct. Mater.*, **5**, 599.
- [16] Sort, J.; Nogués, J.; Amils, X.; Suriñach, S.; Muñoz, J.S; 1999, *Appl. Phys. Lett.*, **75**, 3177.
- [17] Liu, K.; Nogués, J.; Leighton, C.; Masuda, H.; Nishio, K.; Roshchin, I.V.; Schuller, I. K.; 2002, *Appl. Phys. Lett.*, **81**, 4434.

Figure captions:

Figure.1: X-ray diffraction pattern for various samples, showing the presence of Co ((111) peak) & Cr₂O₃ (remaining peaks) phases separately.

Figure.2: HRTEM micrographs of samples A and C.

Figure.3:

a) Partial FC-ZFC hysteresis loops of sample A at 50K (above) and 300K(below); insets show the corresponding complete hysteresis loop from $-2T$ to $2T$ field.

b) Partial FC-ZFC hysteresis loops of sample B at 50K(above) and 300K(below); insets show the corresponding complete hysteresis loop from $-2T$ to $2T$ field.

c) Partial FC-ZFC hysteresis loops of sample C at 50K(above) and 300K(below); insets show the corresponding complete hysteresis loop from $-2T$ to $2T$ field.

d) Partial FC-ZFC hysteresis loops of sample D at 50K(above) and 300K(below); insets show the corresponding complete hysteresis loop from $-2T$ to $2T$ field.

Figure.4: FC (closed circles) and ZFC (open circles), M Vs T curves of samples A, B and D. Field cooling and magnetization measurements were performed in presence of 100 Oe magnetic field.

Table 1: Crystallite size, H_{EB} , $H_C(300K)$, $H_C(50K)$ for different samples.

Sample	Heat treatment H_2	Crystallite size of Co from XRD (St. Dev.)	Crystallite size of Cr_2O_3 from XRD (St. Dev.)	H_{EB} at 50K (Oe)	H_C at 300K (Oe)		H_C at 50K (Oe)	
					FC	ZFC	FC	ZFC
A Series-I	500°C (3hrs)	43nm (3.5)	27.3nm (2.9)	110	192	184	249	209
B Series-I	700°C (15min)	3.1nm (0.4)	3.2nm (0.5)	85	296	270	355	502
C Series-I	700°C (2hrs)	15.4nm (2.4)	35.3nm (3.0)	427	332	324	1037	934
D Series-II	600°C (1hr)	3.3nm (0.6)	4.4nm (0.7)	150	98	104	315	279

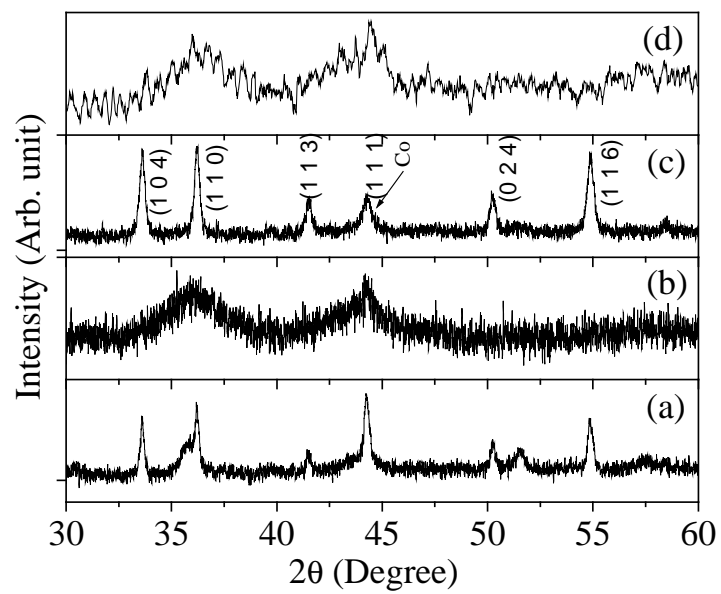


Figure.1

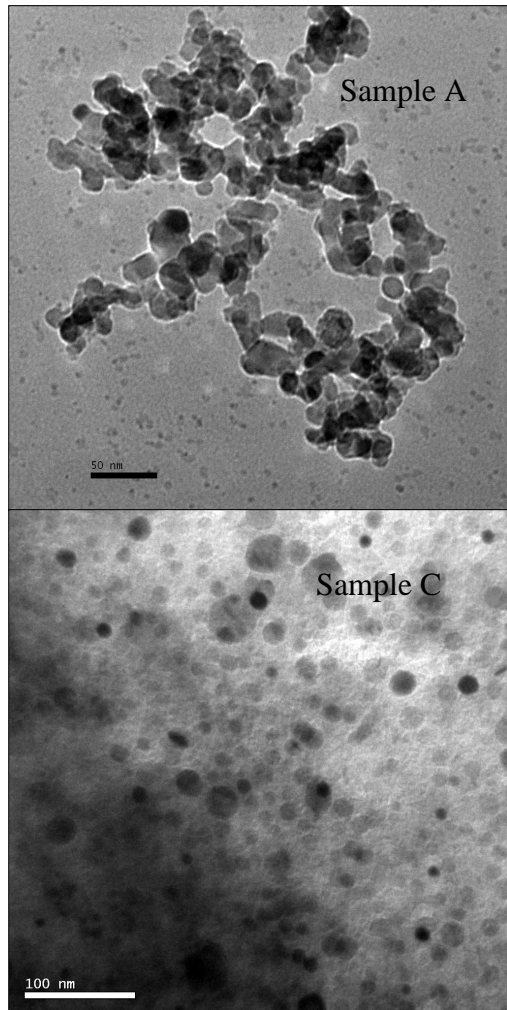


Figure.2

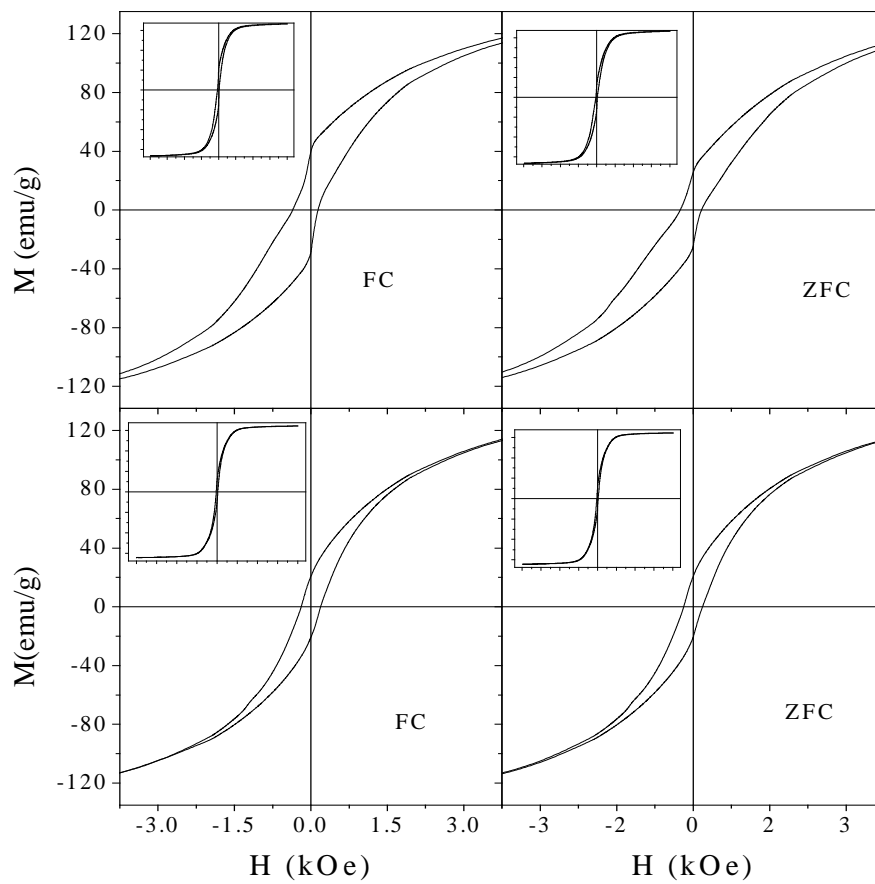


Figure.3a

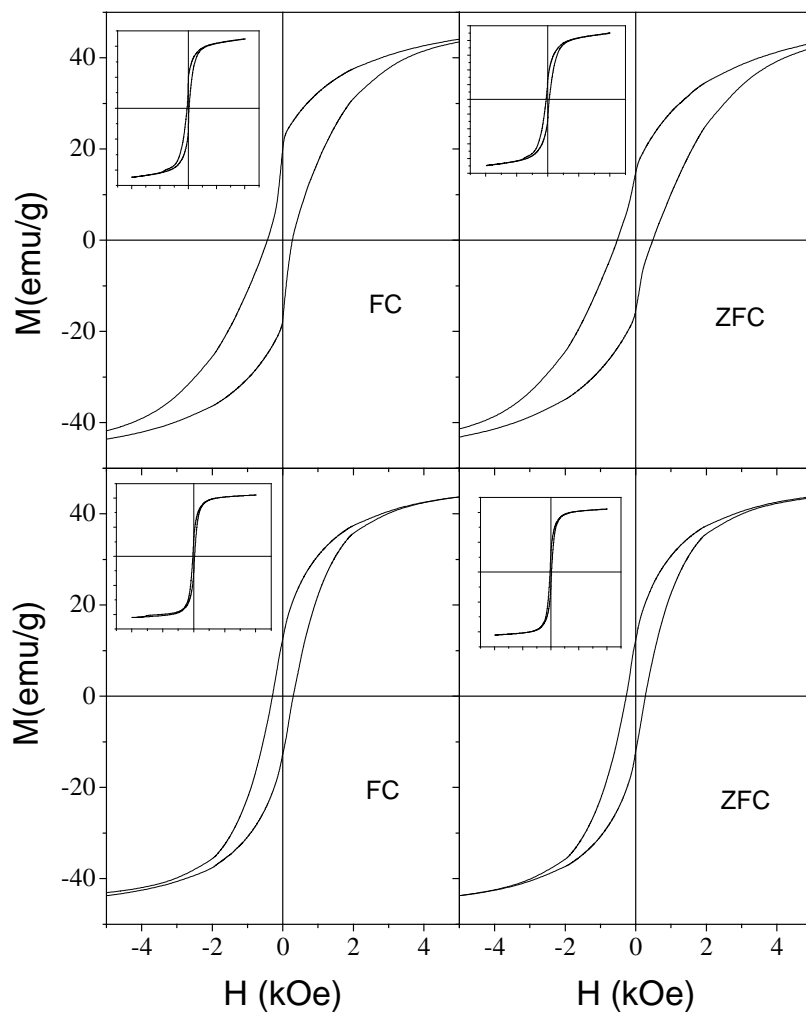


Figure 3b

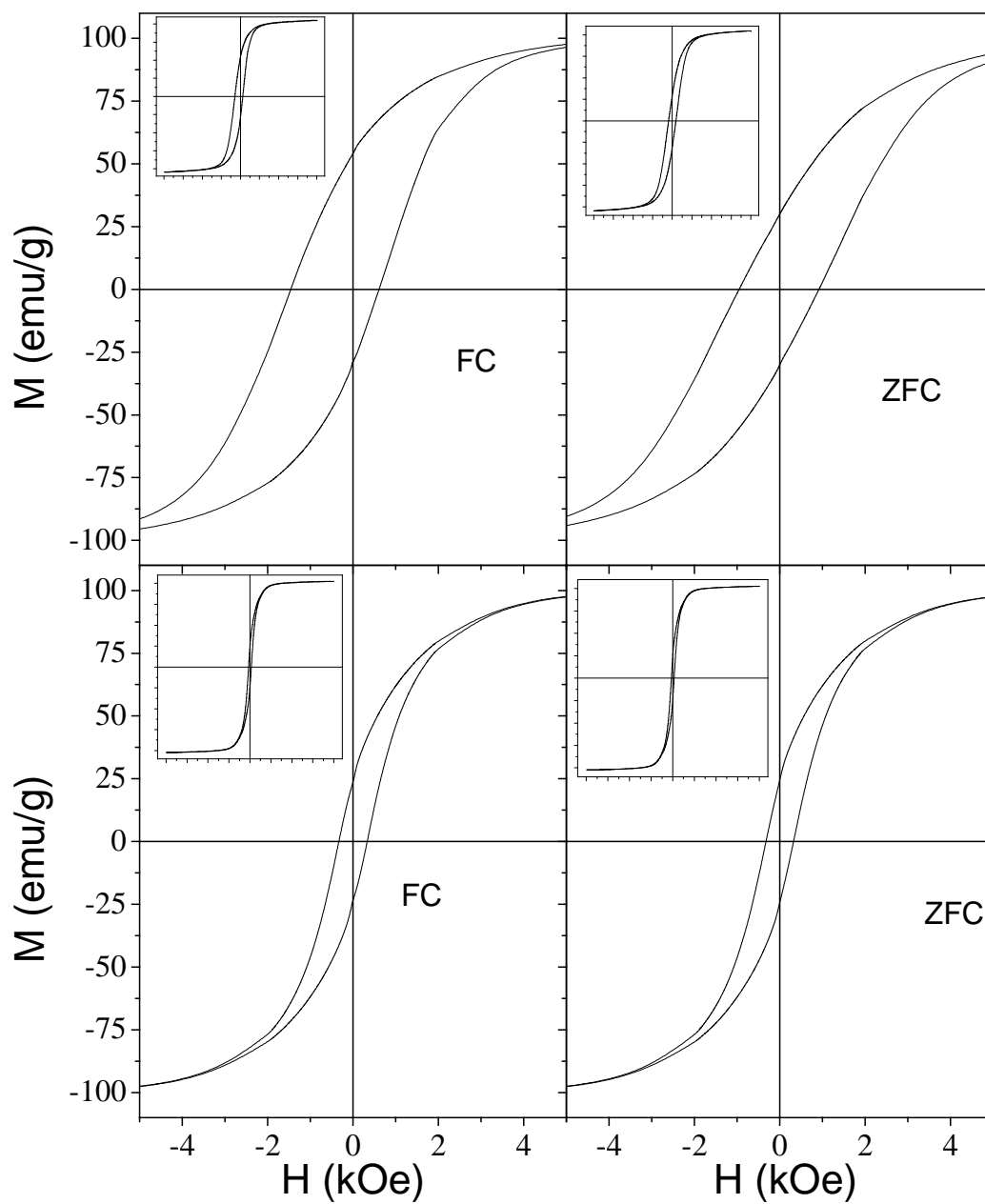


Figure 3c

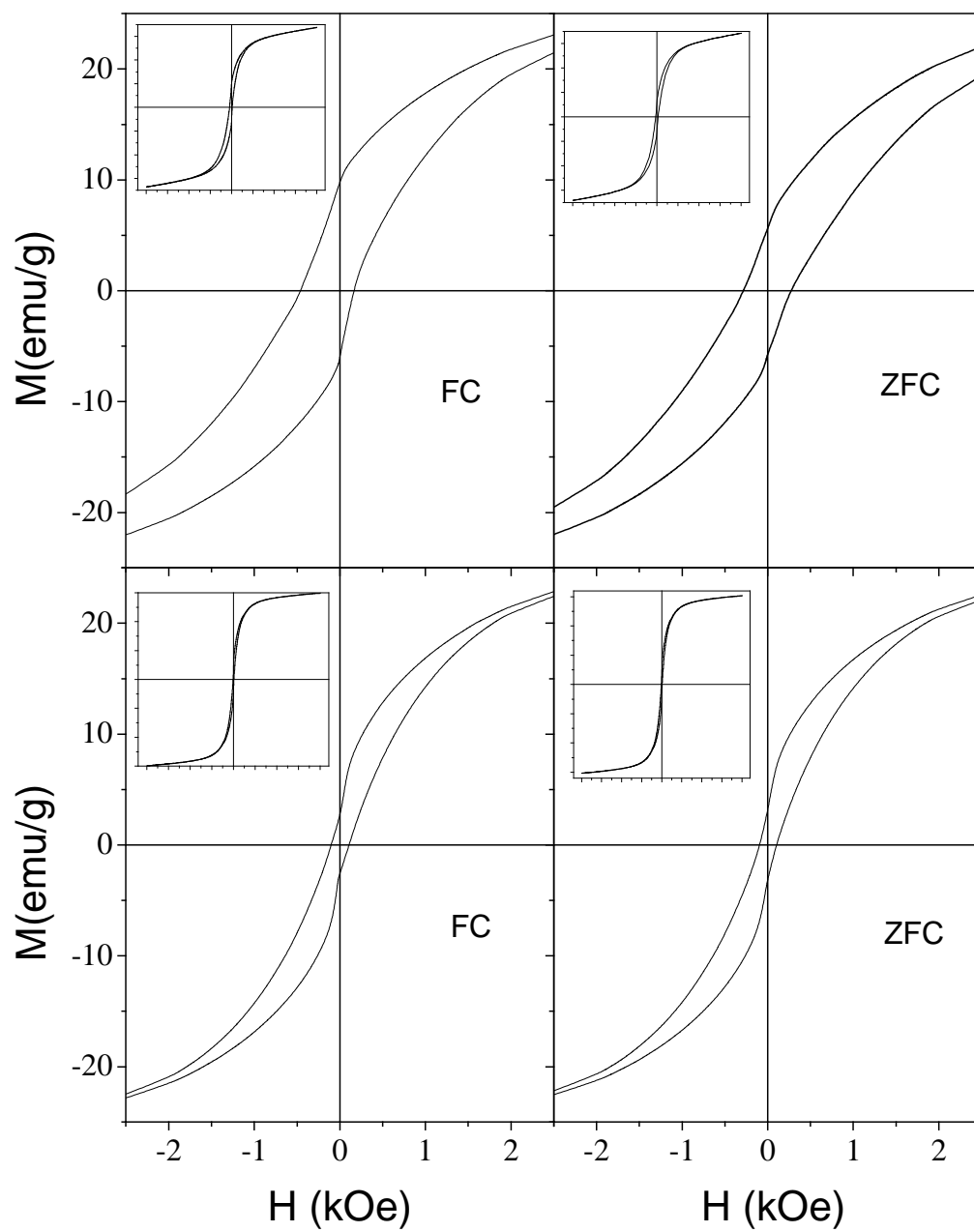


Figure 3d

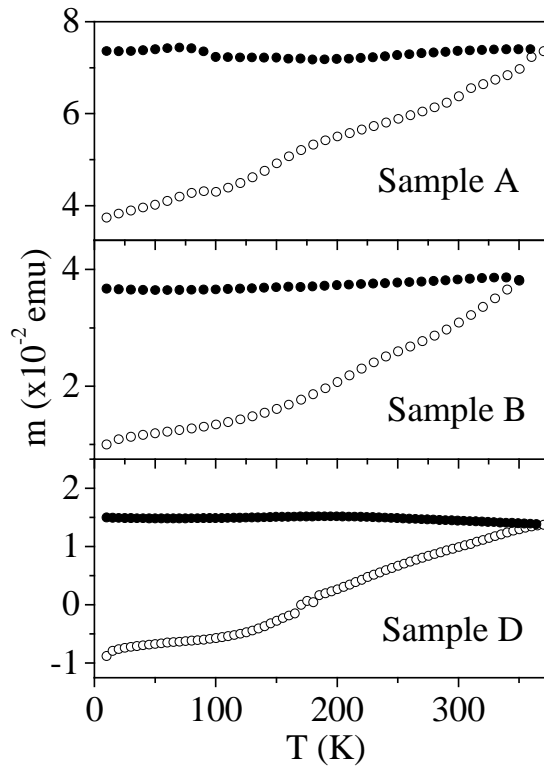


Figure.4